Biogeosciences, 7, 3879–3891, 2010
www.biogeosciences.net/7/3879/2010/
doi:10.5194/bg-7-3879-2010

Biogeosciences

Calcifying invertebrates succeed in a naturally CO_2-rich coastal habitat but are threatened by high levels of future acidification

J. Thomsen[1], M. A. Gutowska[2], J. Saphörster[1], A. Heinemann[1,3], K. Trübenbach[2], J. Fietzke[3], C. Hiebenthal[4], A. Eisenhauer[3], A. Körtzinger[5], M. Wahl[4], and F. Melzner[1]

[1]Biological Oceanography, Leibniz-Institute of Marine Sciences (IFM-GEOMAR), Kiel 24105, Germany
[2]Institute of Physiology, Christian-Albrechts-University Kiel, Germany
[3]Marine Geosystems, Leibniz-Institute of Marine Sciences (IFM-GEOMAR), Kiel 24148, Germany
[4]Marine Ecology, Leibniz-Institute of Marine Sciences (IFM-GEOMAR), Kiel 24105, Germany
[5]Chemical Oceanography, Leibniz-Institute of Marine Sciences (IFM-GEOMAR), Kiel 24105, Germany

Received: 15 June 2010 – Published in Biogeosciences Discuss.: 2 July 2010
Revised: 15 November 2010 – Accepted: 16 November 2010 – Published: 26 November 2010

Abstract. CO_2 emissions are leading to an acidification of the oceans. Predicting marine community vulnerability towards acidification is difficult, as adaptation processes cannot be accounted for in most experimental studies. Naturally CO_2 enriched sites thus can serve as valuable proxies for future changes in community structure. Here we describe a natural analogue site in the Western Baltic Sea. Seawater pCO_2 in Kiel Fjord is elevated for large parts of the year due to upwelling of CO_2 rich waters. Peak pCO_2 values of >230 Pa (>2300 µatm) and pH_{NBS} values of <7.5 are encountered during summer and autumn, average pCO_2 values are ∼70 Pa (∼700 µatm). In contrast to previously described naturally CO_2 enriched sites that have suggested a progressive displacement of calcifying auto- and heterotrophic species, the macrobenthic community in Kiel Fjord is dominated by calcifying invertebrates. We show that blue mussels from Kiel Fjord can maintain control rates of somatic and shell growth at a pCO_2 of 142 Pa (1400 µatm, $pH_{NBS} = 7.7$). Juvenile mussel recruitment peaks during the summer months, when high water pCO_2 values of ∼100 Pa (∼1000 µatm) prevail. Our findings indicate that calcifying keystone species may be able to cope with surface ocean pH_{NBS} values projected for the end of this century when food supply is sufficient. However, owing to non-linear synergistic effects of future acidification and upwelling of corrosive water, peak seawater pCO_2 in Kiel Fjord and many other productive estuarine habitats could increase to values >400 Pa (>4000 µatm). These changes will most likely affect calcification and recruitment, and increase external shell dissolution.

Correspondence to: F. Melzner
(fmelzner@ifm-geomar.de)

1 Introduction

Future ocean acidification will most likely impact ocean ecosystems by differentially modulating species fitness and biotic interactions. Decreases in pH predicted for the next century have been shown to affect several marine taxa (Fabry et al., 2008). In short to intermediate (days to weeks) CO_2 perturbation experiments, calcifying marine invertebrate groups have been shown to react sensitively to simulated ocean acidification (Pörtner et al., 2004; Dupont et al., 2008; Kurihara, 2008). Current hypotheses derived from experimental work suggest that there could be (i) direct effects of carbonate chemistry on calcification rate and shell integrity and that (ii) CO_2 induced disturbances in extracellular acid-base equilibria can lead to metabolic disturbances, which then impact growth and calcification rate, and, ultimately, fitness (Pörtner et al., 2004; Fabry et al., 2008; Melzner et al., 2009).

However, as most laboratory experiments cannot account for species genetic adaptation potential, they are limited in their predictive power. Naturally CO_2 enriched habitats have thus recently gained attention as they could more accurately serve as analogues for future, more acidic ecosystems. The most prominent example, the volcanic CO_2 vents off of Ischia, Italy, have been shown to exert a negative influence on calcifying communities, with certain taxa (scleractinian corals, sea urchins, coralline algae) absent and seagrasses dominating in the acidic parts of the study site (Hall-Spencer et al., 2008). Another study (Tunnicliffe et al., 2009) revealed negative effects of low seawater pH on bivalves (*Bathymodiolus brevior*) living near hydrothermal vents. Shell thickness and daily shell growth increments were reduced when compared to specimens originating from a less impacted site. Additionally, calcification in the low pH

Published by Copernicus Publications on behalf of the European Geosciences Union.

environment was only possible for animals with an intact periostracum and damage of it lead to complete dissolution of carbonate shells.

Upwelling regions could also serve as natural analogue sites. "Corrosive" upwelling of CO_2 enriched Pacific seawater onto the American shelf has recently been demonstrated (Feely et al., 2008). In shelf seas, seasonal stratification of water masses, respiration in deeper layers and subsequent upwelling of CO_2 enriched waters also results in an acidification of coastal surface waters. Our study site in the Western Baltic Sea is such a habitat: summer hypoxia and anoxia develop in bottom water layers, and strong upwelling events have been measured and modelled along the coasts (Hansen et al., 1999; Lehmann et al., 2002). However, prior to this study no detailed measurements of coastal carbonate system variability have been available for this system.

Here, we present first measurements of carbonate system variability in the shallow water habitats of Kiel Fjord. We also present field data on settlement success of invertebrate larvae and discuss growth rates of blue mussels in Kiel Fjord. Further, we conducted two laboratory experiments using the dominant benthic calcifier, the blue mussel *Mytilus edulis*, as a model species. In a first experiment (2 weeks duration), we studied haemolymph ion- and acid base regulation in larger mussels to test whether this species is able to control the carbonate system speciation in its extracellular fluids. In a second experiment (8 weeks duration), we exposed small and medium sized mussels to elevated seawater pCO_2 under an optimized feeding regime to test the hypothesis, whether disturbances in acid-base equilibria impact growth and calcification performance. We analyze shell morphology and microstructure from long-term acclimated mussels in order to determine whether formation of "control" shell material is possible under acidified conditions.

2 Material and methods

2.1 Field study

2.1.1 Determination of carbonate system parameters

Water samples from Kiel Fjord were taken for determination of total alkalinity (A_T) and total dissolved inorganic carbon (C_T). A_T was measured by means of a potentiometric open-cell titration with hydrochloric acid using a VINDTA autoanalyzer (Mintrop et al., 2000; Dickson et al., 2007). C_T was determined coulometrically (Dickson et al., 2007) using a SOMMA autoanalyzer. Both A_T and C_T measurements were measured against Certified Reference Material provided by Andrew Dickson of Scripps Institution of Oceanography (http://andrew.ucsd.edu/co2qc/) to assure accuracy. Measuring duplicate samples yields an overall precision (1 standard deviation) of about $\pm 1\,\mu mol\,kg^{-1}$ and $\pm 1.5\,\mu mol\,kg^{-1}$ for A_T and C_T, respectively. Seawater carbonate system parameters (Ω, pCO_2) were calculated using the CO2sys program (Lewis and Wallace, 1998). Dissociation constants K_1 and K_2 (Mehrbach et al., 1973; Dickson and Millero, 1987), $KHSO_4$ dissociation constant (Dickson, 1990) and the NBS scale [mol kg^{-1} H_2O] were used. Surface pCO_2 values were estimated from weekly measured pH_{NBS} values (42 weeks between 1 April 2008 to 1 April 2009). For this purpose, measured pH_{NBS} was correlated with pCO_2 values calculated from measured A_T and C_T determinations. The resulting linear regression was then used to estimate seawater pCO_2 from pH_{NBS} for weeks in which no water samples for A_T and C_T determinations were taken (N = 9, see Table 1 for A_T and C_T values, $r^2 = 0.94$):

$$pCO2 = -281.14\ pH_{NBS} + 2291.3 \quad (1)$$

where pCO_2 is the seawater pCO_2 in Pa, pH_{NBS} is the measured seawater pH value.

2.1.2 Larval settlement in Kiel Fjord

Between January and November 2008, settlement substrata were exposed monthly to natural colonization at the IFM-GEOMAR pier at a depth of 1 m, approximately 50 m north of the carbonate chemistry sampling site. Settlement substrata were made of grey PVC manually roughed using grain 60 sandpaper to facilitate attachment. Three separate settlement units were used; each consisted of three differently oriented, 5 cm × 5 cm surfaces: vertical, horizontal upwards, horizontal downwards. The units were allowed to rotate freely around their vertical axis. The use of a material well suited for settlement, and the different orientations in space, maximized our capacity to sample a large proportion of the propagules settling in a particular month. After retrieving the substrata at the end of a 4-week-exposure, they were gently rinsed to remove unattached organisms, then foulers were identified to the lowest taxonomic level possible (genus or species), and percent cover per taxon was estimated.

2.1.3 Mussel shell growth using $MnCl_2$ as a marker

Individually tagged young (13 to 22 mm) blue mussels (N = 50) from Kiel Fjord were placed into a net on 31 January 2007 and subsequently submerged into a container containing ambient seawater supplemented with 20 mg l^{-1} $MnCl_2$ for 6 to 24 h (with breaks from 26 July 2007 to 23 August 2007, from 7 November 2007 to 29 November 2007 and from 19 December 2007 to 10 January 2008). In these treatment phases, the mussels incorporated manganese during precipitation of their shells (Barbin et al., 2008). No mortality due to the $MnCl_2$ marking has been observed. The days between the $MnCl_2$ markings the mussel net was freely suspended at the IFM-GEOMAR jetty in Kiel Fjord at about 1 m water depth, enabling the mussels to filter feed in their natural environment. After 12 months (on 05 February 2008) the soft tissue of the mussels

Table 1. Kiel Fjord surface seawater carbonate system speciation 2008 to 2009. See Fig. 1a for corresponding surface pH_{NBS}.

#	Date	S	T (°C)	pH_{NBS}	A_T ($\mu mol\,kg^{-1}$)	C_T ($\mu mol\,kg^{-1}$)	pCO_2 (Pa)	pCO_2 (µatm)	Ω_{calc}	Ω_{arag}
1	2008-07-09	17.4	14.6	7.68	1955.2	1973.1	143	1411	0.79	0.47
2	2008-08-13	16.1	18.7	7.83	1913.7	1891.5	104	1026	1.21	0.72
3	2008-09-08	19.3	15.5	7.49	2044.9	2106.3	234	2309	0.58	0.35
4	2008-10-15	17.3	14.1	7.67	2018.4	2041.3	150	1480	0.79	0.47
5	2008-11-11	21.5	11.5	7.86	2063.3	2037.2	91	898	1.22	0.74
6	2008-12-08	19.6	7.1	7.98	2123.7	2088.2	68	671	1.34	0.80
7	2009-01-12	17.8	3.9	8.01	2078.3	2053.0	62	612	1.18	0.69
8	2009-02-05	16.5	3.3	8.10	2113.2	2075.3	52	513	1.36	0.79
9	2009-03-05	14.5	3.5	8.23	2067.7	2008.3	39	385	1.67	0.96

Speciation of the carbonate system in Kiel Fjord surface water

was removed and the left valve of one individual (initial shell length: 16.1 mm, final shell length: 46.6 mm) was prepared for electron micro probe (EMP) measurements: the shell was cut along the axis of maximum growth using a cut-off wheel and shell sections were embedded in a two component epoxy resin (Buehler, EPO-THIN, Low Viscosity Epoxy Resin) on a brass-slide. After hardening at 50 °C, the sections were ground with sand paper (grading (p): 240 to 600) and polished with diamond paste (grading 0.5 to 0.01 µm). EMP analyses were performed using a JEOL JXA 8200 "Superprobe" applying Wavelength Dispersive Spectrometry (WDS), using a focused beam, a resolution between 3 µm×3 µm and 10 µm×10 µm and an integration time per point of 400 ms.

2.2 Laboratory experiments

2.2.1 Animals

Mytilus edulis was collected from a subtidal population in Kiel Fjord (54°19.8′ N; 10°9.0′ E, see Nikulina et al., 2008 for a detailed map of the study site). For extracellular acid-base status experiments (Exp. 1), large specimen with a shell length of 76 ± 5 mm were used. The long-term growth and calcification trial (Exp. 2) was conducted with mussels of 5.5 ± 0.6 ("small") and 13.3 ± 1.4 mm ("medium") shell length. Mussels were collected in March and April 2008 (acid-base regulation) and May 2009 (growth and calcification). Prior to experimentation, shells were cleaned of epibionts and animals were acclimated to the experimental settings for one to two weeks.

2.2.2 Experimental setup

Experiments were performed in a flow-through seawater system under a 14:10 hours light:dark cycle. Seawater from Kiel Fjord was filtered through a series of 50, 20, and 5 µm filters, UV-sterilized and subsequently pumped at a rate of $5\,l\,min^{-1}$ into a storage tank of 300 l. The water was aerated and mixed by a pump to ensure that air saturated water was pumped up to a header tank which supplied 12 experimental aquaria (16 l each) by gravity feed. The flow rate was adjusted to $100\,ml\,min^{-1}$ in each aquarium. Overflow drain pipes in the storage tank, header tank, and every aquarium ensured constant water levels in the system. The experimental aquaria were continuously aerated using a central automatic CO_2 mixing-facility (Linde Gas & HTK Hamburg, Germany). This custom built gas-mixing facility determines the CO_2 content of inflowing ambient air and automatically adds pure CO_2 to produce five different CO_2-air mixtures. CO_2-enriched air with a pCO_2 of 560, 840, 1120, 1400 and 4000 ppmv was injected into the experimental aquaria at a rate of $0.8\,l\,min^{-1}$ using aquarium diffuser stones (Dohse, Grafschaft-Gelsdorf, Germany). Ambient air (ca. 385 ppm pCO_2) was used as a control.

2.2.3 Experimental protocol

Experiment 1

Two *M. edulis* experimental runs lasted for 14 d each at a constant water temperature of 12 °C. Temperature in the storage tank was kept constant using heaters (Eheim, Deizisau, Germany) or a flow-through cooler (TITAN 1500, Aqua Medic, Bissendorf, Germany). In the first run (Exp. 1a, 29 April to 16 May 2008) only the five lower pCO_2 levels were used, in the second run (Exp. 1b, 28 May to 12 June 2008) all six levels were used. Six mussels were placed in each of the experimental aquaria (total wet mass per aquarium was 246 ± 35 g). Mussels were fed with a suspension of algae (DT's Live Marine Phytoplankton Premium Blend, Rebie, Germany) which was pumped into the header tank using a peristaltic pump at a rate of $1\,ml\,min^{-1}$ to maintain stable concentrations of 1000 to 4000 cells ml^{-1} in the experimental aquaria. Previous work established that blue mussels display maximum filtration rates when exposed to such algal densities (Riisgard et al., 2003). The algae suspension contained *Nannochloropsis oculata* (40%), *Phaeodactylum*

tricornutum (40%), and *Chlorella* sp. (20%). At the end of the experimental period, the animals were gently removed from the aquaria. Extracellular fluid samples were taken within 2 min after removal from the aquaria. Haemolymph samples of *M. edulis* were drawn anaerobically with a syringe from the posterior adductor muscle after the valves were opened and blocked with a pipette tip. Two samples were taken from each animal. The first sample (200 µl) was used for pH determination and the second (500 µl) for measurement of total dissolved inorganic carbon (C_T) and ion composition (see below). Water samples were taken from the aquaria for the determination of ionic composition, A_T, and C_T. Similarly to haemolymph samples, extrapallial fluid (EPF) was sampled from the extrapallial space by gently inserting a syringe needle between shell and the pallial attachment. For comparison of EPF and haemolymph acid-base status, mussels were sampled from the field on 30 August 2010. Prior to measurements, mussels were stored in a flow-through aquarium to avoid sampling stress artefacts.

Experiment 2

In a long-term growth experiment, mussels were exposed for 2 months to three pCO_2 levels (39, 142, and 405 Pa or 385, 1400, 4000 µatm) in four replicate aquaria for each treatment level at a mean temperature of 13.8 ± 0.6 °C between 14 May to 13 July 2009. Each replicate contained 8 mussels of 5.5 mm ("small") and 13 mm ("medium") shell length. Initial total biomass per replicate aquarium was 14 ± 0.5 g. Mussels were continuously fed with a *Rhodomonas* sp. suspension containing 2903 ± 1194 cells ml^{-1} which was introduced into each aquarium at a rate of 100 ml min^{-1}. *Rhodomonas* sp. was cultured in 0.2 µm filtered seawater enriched with Provasoli seawater (PES) medium (Ismar et al., 2008), phosphate, and nitrate at a final concentration of 0.036 mmol l^{-1} P and 0.55 mmol l^{-1} N in plastic bags at 7.5 l each under constant illumination. Mean algae concentrations in the experimental aquaria were 820 ± 315 cell ml^{-1}. Shell length and fresh mass of the mussels were measured at the beginning of the experiment and after 8 weeks using a calliper (± 0.1 mm) and a precision balance (± 1 mg). Somatic dry and shell mass were measured after drying the animals for 24 h at 80 °C using a precision balance (± 1 mg, Sartorius, Germany). Similar determinations were carried out for control mussels from Kiel Fjord collected at the sampling site of our experimental animals.

2.2.4 Monitoring of the carbonate system

Daily measurements of pH, salinity, and temperature were performed in the aquaria pH_{NBS} was measured with a WTW 340i pH-meter and a WTW SenTix 81-electrode which was calibrated with Radiometer IUPAC precision pH buffer 7 and 10 (S11M44, S11 M007) on the National Bureau of Standards (NBS) scale. Salinity and temperature were measured with a WTW cond 315i salinometer and a WTW TETRACON 325 probe. Additionally, water samples for A_T and C_T measurements were taken from the aquaria and analyzed as mentioned in Sect. 2.1.1.

2.2.5 Determination of extracellular acid-base and ion status

In experiment 1, *M. edulis* haemolymph (HL) pH_{NBS} was measured in a 12 °C water bath using fiber-optic sensors (optodes, PreSens, Regensburg, Germany) which were installed in the tip of 1 ml syringes (Gutowska and Melzner, 2009). Samples were filtered through a glassfiber filter at the syringe tip to remove haemocytes. The sensors were calibrated in ambient sea water which was adjusted to four different pH_{NBS} values between 6.9 and 7.8 with HCl and NaOH. Optodes were calibrated against a WTW 340i pH meter and a SenTix 81 electrode, calibrated with Radiometer precision buffers (S11M44, S11 M007). For comparison of haemolymph and extrapallial pH samples were measured within a cap using a microelectrode (WTW Mic-D) and a WTW 340i pH meter. The slight offset of the WTW pH_{NBS} electrodes with respect to pH_{NBS} values calculated from A_T and C_T measured on the same water samples were corrected by using the following linear relationship (Eq. (2), N = 95, $r^2 = 0.96$):

$$\text{pH corrected} = 0.9398\ \text{pH measured} + 0.556 \quad (2)$$

Haemolymph C_T was measured in two 100 µl subsamples with a Corning 965 CO_2 analyzer. To correct for instrument drift, 100 µl of distilled water were measured prior to each determination. Thus, a precision and accuracy of 0.1 mmol l^{-1} could be reached. To determine in vitro non-bicarbonate buffer (NBB) – values of extracellular fluid, 600 µl samples pooled from 10 animals were equilibrated with humidified CO_2 gas mixtures (pCO_2 57, 142, 405, 564 Pa or 560, 1400, 4000, 5570 µatm) for 1 h using the gas mixing facility and a gas mixing pump (Wösthoff, Bochum, Germany). Incubations were performed in a shaking water bath at 12 °C, using glass flasks (120 ml) as incubators. pH_{NBS} and C_T were measured using a microelectrode (WTW Mic-D) and Corning 965 CO_2 analyzer, respectively, as described above.

Body fluid pCO_2, bicarbonate, and carbonate concentrations were calculated from measured pH_{NBS} and C_T values according to the rearranged versions of the Henderson-Hasselbalch equation:

$$pCO_2 = C_T \left(10^{pH - pK'_1} \alpha CO_2 + \alpha CO_2\right)^{-1} \quad (3)$$

$$\left[HCO_3^{2-}\right] = 10^{pH - pK'_1} \alpha CO_2\, pCO_2 \quad (4)$$

$$\left[CO_3^{2-}\right] = 10^{pH - pK'_2} \left[HCO_3^-\right] \quad (5)$$

where α is the CO_2 solubility coefficient and pK'_1 and pK'_2 are the first and second apparent dissociation constants of carbonic acid. α_{CO_2} (Weiss, 1974) and pK'_2 (Roy et al., 1993) were chosen according to experimental temperature and salinity. pK'_1 was calculated from pH_{NBS}, C_T, and pCO_2 measured in vitro in the body fluid using Eq. (6) (Albers and Pleschka, 1967):

$$pK'_1 = \mathrm{pH} - \log\left(\frac{C_T}{pCO_2\,\alpha CO_2} - 1\right) \quad (6)$$

A linear relationship was found for pK'_1 in relation to pH_{NBS}. The regression for pK'_1 for *M. edulis* haemolymph was $pK'_1 = -0.1795\ pH_{NBS} + 7.5583$ ($r^2 = 0.5$). The calculated values for pK'_1 varied between 6.20 ± 0.03 in control and 6.27 ± 0.02 in 405 Pa (4000 µatm) pCO_2 treated animals. Protein concentration in the haemolymph was determined using a Thermo Multiskan spectrum photometer (Waltham, Massachusetts, USA) and BSA standard solutions (Bradford, 1976). Prior to measurements, samples were centrifuged to remove haemocytes (100 g, 25 min, 2 °C). The total cation concentrations of water and body fluid were measured using a Dionex ICS-2000 ion chromatograph, a CS18 column and methane sulfonic acid as eluent. Samples were centrifuged for 20 min at 100 g and 4 °C to remove haemocytes. The supernatant was transferred into a new cap and frozen at −20 °C. Prior to measurement, body fluid and ambient seawater samples were diluted 1:100 with deionized water. A calibration curve was obtained by measuring a dilution series of 1:50, 1:100, 1:200, 1:300, 1:400, and 1:500 of the IAPSO seawater standard (International Association for the Physical Sciences of the Oceans, batch: P146; 12 May 2005; salinity: 34.992; K15: 0.99979).

2.2.6 Shell morphology and shell microstructure

Shell morphology was assessed for 20 randomly chosen, medium sized mussels from each treatment in experiment 2. Mussel shells were checked for external and internal shell dissolution under low magnification (8 fold magnification) using a stereomicroscope. Shell umbones were photographed at 18 times magnification and analyzed for signs of external dissolution (50 fold magnification). Images were analyzed for the extent of dissolution at the umbo with an accuracy of 1 mm^2 (the large uncertainty is due to the curvature of the shell). The severity of dissolution was graded according to a "dissolution index" scale: 0 = no dissolution, 1 = periostracum abrasion, 2 = calcite dissolution visible, 3 = massive dissolution of calcite, multi – layered, often with round dissolution pits. Other dissolution spots on the outer shell surface were not quantified.

The microstructure of shell cross sections at two different positions of the shell of randomly chosen *M. edulis* (N = 5) from experiment 2 (medium size) of similar final shell lengths was investigated. Shells were perforated every 2 mm along the longitudinal axis (i.e. anterior-posterior axis) using a 1 mm diameter drill. They could then be manually fractured in a controlled fashion. Shell analysis was performed exclusively on intact cross sections between drilled holes. Such a procedure produces high quality cross sections. Position 1 (at 75% shell length) is located anterior to the pallial line (PL) and consists of aragonite and calcite layers. Position 2 (at 95% shell length) lies posterior to the PL and is solely composed of calcite. Both positions are located in shell regions formed during the experiment. The shell fractions were coated with gold-palladium and examined using scanning electron microscopy (SEM, Nanolab 7, Zeiss). The thickness of the different crystal layers (calcite and aragonite) and the number of the aragonite platelets were quantified.

2.3 Statistical analyses

Regression analysis was performed with SigmaPlot 10. Statistical analyses were performed using STATISTICA 8. Differences between treatments were analyzed using one- and two-way ANOVA and the Tukey post-hoc test for unequal N. Relative quantities were arcsine transformed prior to analysis. For shell morphology analysis of dissolved shell area and the dissolution index, non-parametric Kruskal-Wallis and subsequent Dunn's multiple comparisons tests were used. Values in graphs and tables are means ± standard deviation. See the caption of Table S1 for more information on statistical tests used.

3 Results and discussion

3.1 Habitat carbonate system speciation and calcifying communities

The western Baltic Sea is characterized by low salinity (10 to 20) and relatively low A_T of 1900 to 2150 µmol kg^{-1}. Thus, the calcium carbonate saturation state (Ω) typically is much lower than in the open ocean. The A_T and C_T measurements in 2008 and 2009 indicate that Ω_{arag} did not exceed a value of 1 in Kiel Fjord surface waters during summer and autumn. Even Ω_{calc} dropped below one on multiple occasions (Table 1). Minimum values for Ω_{arag} (Ω_{calc}) were 0.35 (0.58) in September 2008. Low Ω is associated with high surface pCO_2 during the summer and autumn months, caused by upwelling of CO_2-rich deep water masses (Hansen et al., 1999). Kiel Fjord surface pCO_2 exceeds present average ocean pCO_2 values during large parts of the year. Habitat pCO_2 varies between 38 and 234 Pa (375 and 2309 µatm), pH_{NBS} varies between 7.49 and 8.23. Using a correlation of weekly measured surface pH_{NBS} and calculated pCO_2 from A_T and C_T measurements, we estimate that in 34%, 23% and 9% of the 42 weeks investigated, pCO_2 exceeded pre-industrial pCO_2 (28 Pa, 280 µatm) by a factor of three (>85 Pa, >840 µatm), four (>113 Pa, >1120 µatm) and five (>142 Pa, >1400 µatm), respectively.

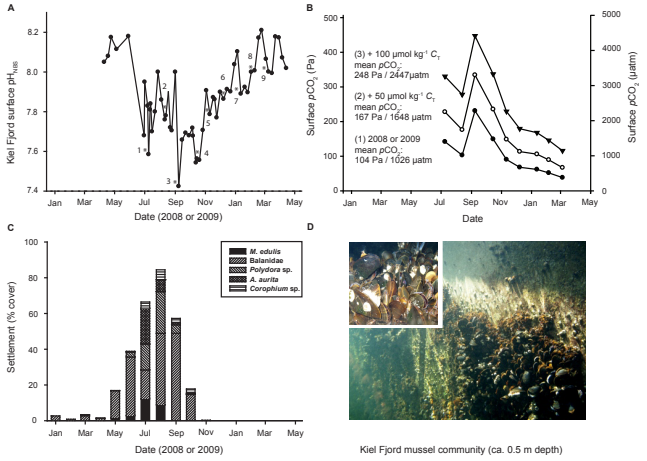

Fig. 1. **(A)** Surface pH_{NBS} in Kiel Fjord at the site of the experimental mussel population (54° 19.8′N; 10° 9.0′E) in 2008 and 2009. Stars and numbers indicate dates for which accurate determinations of total alkalinity (A_T) and dissolved inorganic carbon (C_T) are available, see Table 1. **(B)** Kiel Fjord pCO_2 replotted from Table 1, and calculated after addition of 50 (2) and 100 (3) µmol kg^{-1} of C_T to C_T from Table 1. A doubling in surface pCO_2 will result in an increase in C_T by about 90 µmol kg^{-1} in this habitat (see text). **(C)** Settlement of marine invertebrates on vertically suspended PVC plates. Plates (N = 3 each) were exchanged monthly and epibionts were quantified. **(D)** Image of typical vertical hard substrate in Kiel Fjord dominated by calcifying communities.

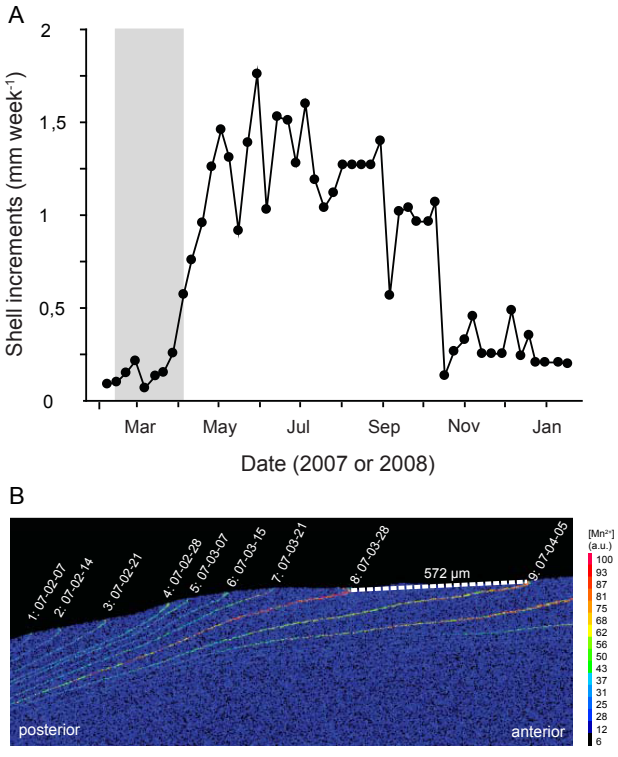

Fig. 2. Manganese marks in the calcite of the shell of a wild *Mytilus edulis* from Kiel Fjord illustrating weekly shell length growth between 7 February 2007 (line 1) and 5 April 2008 (line 9). Shell $[Mn^{2+}]$ in arbitrary units (a.u).

Given the characteristics of the carbonate system, it is surprising that blue mussel (*Mytilus edulis*) beds and associated calcifying benthic species (e.g. the barnacle *Amphibalanus improvisus* and the echinoderm *Asterias rubens*) are common features in Kiel Fjord and the Western Baltic. *M. edulis* forms a shell consisting of an inner aragonite (nacre) and outer calcite layer, covered and protected by an organic layer, the periostracum. Despite an extensive organic matrix surrounding the calcite and aragonite crystals, 95–99.9% of the shell's mass is made of $CaCO_3$ (Yin et al., 2005). *M. edulis* constitutes more than 90% of the macrofauna biomass in many habitats in the Western Baltic (Reusch and Chapman, 1997; Enderlein and Wahl, 2004). Competitive dominance is achieved primarily through very high rates of recruitment (spat fall) and high rates of juvenile growth (Dürr and Wahl, 2004). Previous results indicate that *M. edulis* (2 to 3 cm shell length) are characterized by shell growth rates of ca. 4 mm $month^{-1}$ during the summer months in Kiel Fjord (Kossak, 2006). Our EMP analysis of a $MnCl_2$ marked mussel confirms these earlier findings and indicates that weekly shell increments in the field can exceed 1 mm $week^{-1}$ between May and October (Fig. 2). The settlement of juvenile mussels in 2008 occurred when highest pCO_2 values were encountered in the habitat (Fig. 1c): peak settlement took place in July and August, at an average surface pCO_2 of 98 Pa (967 µatm). Other calcifying invertebrates (e.g. the barnacle *Amphibalanus improvisus*) also settled abundantly between May and October 2008 in Kiel Fjord (Fig. 1c). When settlement plates are not exchanged regularly, mussels dominate the species assemblage (99% of the biomass) in Kiel Fjord within ∼10 weeks in summer (Enderlein and Wahl, 2004).

3.2 Extracellular acid-base status (Exp. 1)

In order to better understand the success of *M. edulis* in Kiel Fjord, a chemically and physiologically challenging habitat, we studied the haemolymph pH_{NBS} (pH_e) and ion regulation (Exp. 1) and, subsequently growth and calcification performance (Exp. 2). Mussels do not regulate pH_e when exposed to elevated pCO_2. pH_e followed the non-bicarbonate buffer line when displayed in a Davenport–diagram (Fig. 3, Table 3), suggesting that buffering by extracellular proteins (1.2 ± 0.4 mg ml^{-1}, N = 8 control mussels) is the sole mechanism to stabilize pH_e. The buffer value of the haemolymph is low (0.49 mmol HCO_3^- l^{-1} pH^{-1}, Fig. 3), matching findings from other populations of the same species (Booth et al., 1984; Lindinger et al., 1984). Significant reductions in pH_e were found at 142 and 405 Pa (1400 and 4000 µatm) (Table 3, Fig. 3a). No significant changes in the concentration

Table 2. Seawater carbonate system speciation during experimental trials (mean ± SD, 14 and 3 determinations for pH, S, T and A_T, C_T). Salinity (S) was 11.8 ± 0.4 and temperature (T) 12.5 ± 0.5 °C in Exp. 1 (duration 2 weeks), $S = 15.0 \pm 0.6$ and $T = 13.8 \pm 0.6$ °C in Exp. 2 (duration: 8 weeks).

Exp. 1:							
Treatment	pH_{NBS}	A_T (µmol kg^{-1})	C_T (µmol kg^{-1})	pCO_2 (Pa)	pCO_2 (µatm)	Ω_{calc}	Ω_{arag}
39 Pa	8.05	1901,4	1841.5	47	464	1.77	1.01
385 µatm	±0.03	±42,2	±36.2	±2	±20	±0.13	±0.08
57 Pa	7.89	1903,5	1873.5	67	661	1.31	0.75
560 µatm	±0.04	±40,8	±31.3	±5	±49	±0.16	±0.09
85 Pa	7.81	1905,6	1891.8	80	789	1.09	0.62
840 µatm	±0.03	±40,3	±34.7	±3	±30	±0.09	±0.05
113 Pa	7.70	1906,2	1914.3	106	1046	0.86	0.49
1120 µatm	±0.03	±38,9	±34.1	±5	±49	±0.07	±0.04
142 Pa	7.56	1906,1	1943.9	150	1480	0.64	0.37
1400 µatm	±0.06	±39,3	±53.7	±31	±306	±0.09	±0.05
405 Pa	7.08	1890,8	2077.5	431	4254	0.22	0.12
4000 µatm	±0.02	±25,1	±12.0	±35	±345	±0.01	±0.01
Exp.: 2							
Treatment	pH_{NBS}	A_T (µmol kg^{-1})	C_T (µmol kg^{-1})	pCO_2 (Pa)	pCO_2 (µatm)	Ω_{calc}	Ω_{arag}
39 Pa	8.13	1966.1	1891.2	50	493	1.94	1.14
385 µatm	±0.02	±3.2	±5.3	±3	±29	±0.04	±0.04
142 Pa	7.72	1968.1	1984.4	135	1332	0.81	0.48
1400 µatm	±0.06	±4.9	±12.3	±20	±197	±0.09	±0.06
405 Pa	7.26	1970.2	2125.8	395	3898	0.28	0.17
4000 µatm	±0.04	±4.3	±12.6	±22	±217	±0.02	±0.01

Seawater carbonate system speciation during experimental trials.

of haemolymph Mg^{2+} and Ca^{2+} were observed with respect to treatment pCO_2 (Table 3). While it was proposed that mytilid mussels use HCO_3^- derived from their shells to buffer pH_e (Lindinger et al., 1984; Michaelidis et al., 2005), our results clearly demonstrate that in flow-through seawater experimental designs, *M. edulis* do not maintain extracellular $[HCO_3^-]$ above that of ambient seawater. This is in contrast to the more active cephalopod molluscs which greatly elevate extracellular $[HCO_3^-]$ in order to stabilize pH_e to conserve haemocyanin blood oxygen transport (Gutowska et al., 2010). However, while *M. edulis* does not possess a pH sensitive respiratory pigment, uncompensated pH_e might negatively impact shell formation: comparing control extracellular pH of haemolymph drawn from the posterior adductor muscle with that of the extrapallial fluid (EPF), the fluid that fills the space between mantle and shell surface, indicates that both fluids are characterized by a very similar carbonate system speciation (Table 3b). Assuming that pH_e in the EPF always behaves like that of haemolymph, it is very likely that the inner shell layers (nacre), which primarily consist of aragonite, are in contact with a fluid that is highly under saturated with $CaCO_3$: $[CO_3^{2-}]$ is much lower in the haemolymph than in seawater at seawater pCO_2 values 142 Pa and lower (see Fig. 3b). In addition, as only 15% of total EPF $[Ca^{2+}]$ has been found to be freely dissolved Ca^{2+} (Misogianes and Chasteen, 1979), Ω_{arag} would be even lower at the inner shell interface. Therefore, even under control conditions at high seawater pH, calcification proceeds in a high pCO_2 compartment. This fact and the high Mg^{2+} concentrations in the EPF accentuate the importance of a microenvironment at the site of calcification suitable to facilitate precipitation of calcium carbonate. Recent findings suggest that proteins with $CaCO_3$ and chitin binding domains (Pif 80 and Pif 97) are excreted from the mantle tissue in a bivalve (Suzuki et al. 2009). Given that the situation is similar in *M. edulis*, proteins could bind to the chitinous layers secreted by the mantle between successive aragonite layers to form micro-compartments, in which the calcification process occurs, potentially in a medium that is different in carbonate chemistry from that of the bulk EPF fluid (see Weiss, 2010). Still, once the aragonite platelets are formed, they are in contact with the EPF. It is not fully clear to what degree the EPF facing aragonite layers are protected by organic matrix against a fluid that is severely undersaturated with $CaCO_3$ at low seawater pCO_2.

Table 3. (A) Exp. 1 haemolymph acid-base status and ion concentrations of large mussels in relation to treatment pCO_2. Significant differences from control (39 Pa, 385 µatm treatment) in bold, mean values ± SD. (B) Haemolymph (HL) vs. extrapallial fluid (EPF) acid-base status in 11 mussels sampled from Kiel Fjord at an ambient seawater pCO_2 of 50 Pa (493 µatm) (30 August 2010) at T = 15.7 °C, S = 14.6, pH_{NBS} = 7.89 during the main growth period in this habitat.

(a) experimental animal haemolymph acid-base status

Treatment (Pa / µatm)	pH_{NBS}	$[HCO_3^-]$ (mmol l^{-1})	$[CO_3^{2-}]e$ (µmol l^{-1})	pCO_2e (Pa)	pCO_2e (µatm)	$[Na^+]e$ % of SW	$[K^+]e$ % of SW	$[Mg^{2+}]e$ % of SW	$[Ca^{2+}]e$ % of SW
39 Pa	7.59	1.77	24.6	169.7	1675	100.9	128.9	104.4	110.5
385 µatm	±0.16	±0.15	±7.6	±76.7	±757	±1.9	±15.2	±2.0	±6.7
57 Pa	7.53	1.78	22.4	171.8	1694	99.4	117	102	103.6
560 µatm	±0.15	±0.13	±7.4	±90.6	±894	±4.4	±10.3	±6.2	±5.7
85 Pa	7.54	1.61	20.5	175.3	1730	103.3	120.7	105.9	109.1
840 µatm	±0.17	±0.13	±8.7	±78.9	±779	±5.9	±18.2	±6.0	±8.4
113 Pa	7.43	1.79	18	243.6	2404	102.5	130.4	102.7	106.3
1120 µatm	±0.12	±0.30	±8.0	±75.1	±741	±2.7	±7.3	±5.4	±5.4
142 Pa	**7.36**	1.64	**13.6**	272	2684	102.9	130.4	103.6	110.3
1400 µatm	± **0.11**	±0.17	± **2.4**	±99.3	±980	±2.4	±25.9	±5.4	±4.2
405 Pa	**7.16**	1.81	**9.8**	**496**	**4895**	**108.2**	134.8	108.2	113.1
4000 µatm	± **0.09**	±0.35	± **3.9**	± **31.8**	± **314**	± **1.3**	±11.5	±1.2	±2.6

(b) haemolymph (HL) vs. extrapallial fluid (EPF) acid-base status in field animals

Fluid	pH_{NBS}	$[HCO_3^-]$ (mmol l^{-1})	$[CO_3^{2-}]e$ (µmol l^{-1})	pCO_2e (Pa)	pCO_2e (µatm)
HL	7.55	1.74	29	174	1740
	±0.08	±0.17	±7	±17	±174
EPF	7.52	1.78	27	179	1785
	±0.10	±0.14	±7	±14	±139

(Exp. 1): Extracellular acid-base and ion status in haemolymph (HL) and extrapallial fluid (EPF).

3.3 Growth and calcification (Exp. 2)

To estimate the long-term consequences of decreased pH_e on the energy budget and the calcification machinery, a growth experiment under optimized feeding conditions was performed (Exp. 2). Previous studies suggested that, in mytilid bivalves (*M. galloprovincialis)*, uncompensated reductions in pH_e may be causally related to reductions in metabolism (metabolic depression) and somatic growth (Michaelidis et al., 2005). In the 8 week growth study, shell growth was high under control conditions (3.3 to 4.6 mm month^{-1} in small vs. medium mussels), fully matching summer field growth rates for mussels of the same size class in Kiel Fjord (Kossak, 2006). Initial mussel shell length and pCO_2 had significant effects on the linear extension of the shell and shell mass increment (see Table S1 for ANOVA results). While the shell mass and extension rate were similar in control and 142 Pa (1400 µatm) treated medium sized mussels, both parameters were significantly reduced at 405 Pa (4000 µatm) (Fig. 4a). In the smaller size group, length growth was significantly reduced at 405 Pa (4000 µatm) as well. There were no significant differences in shell mass growth in small mussels, although a trend towards lower shell mass was apparent in the 405 Pa (4000 µatm) group as well (Fig. 4b). However, when displaying shell mass vs. shell length in comparison to wild-type mussels collected from the sampling site in Kiel Fjord (grey symbols in Fig. 4a and b), it appears that all experimental groups lie within the 95% prediction band of the shell mass vs. length function. This indicates that exposure to elevated pCO_2 does not result in the production of an abnormal, thinner shell phenotype; rather, shell growth is slowed down proportionally. Regardless of the decreased rates of shell growth at higher pCO_2 (405 Pa), all mussels increased their shell mass at least by 150% during the 8 week trial, even at Ω_{arag} (Ω_{calc}) as low as 0.17 (0.28) (Fig. 4e). This is in contrast to a previous study that has suggested a high sensitivity of mussel calcification to elevated pCO_2: during acute exposure, a linear correlation between $CaCO_3$ precipitation rate and seawater pCO_2 (and $[CO_3^{2-}]$) has been observed in *M. edulis* from the Western Scheldt (Gazeau et al., 2007). A reduction in calcification by about 50% was found at a pCO_2 of ca. 100 Pa (ca. 1000 µatm), net shell dissolution was

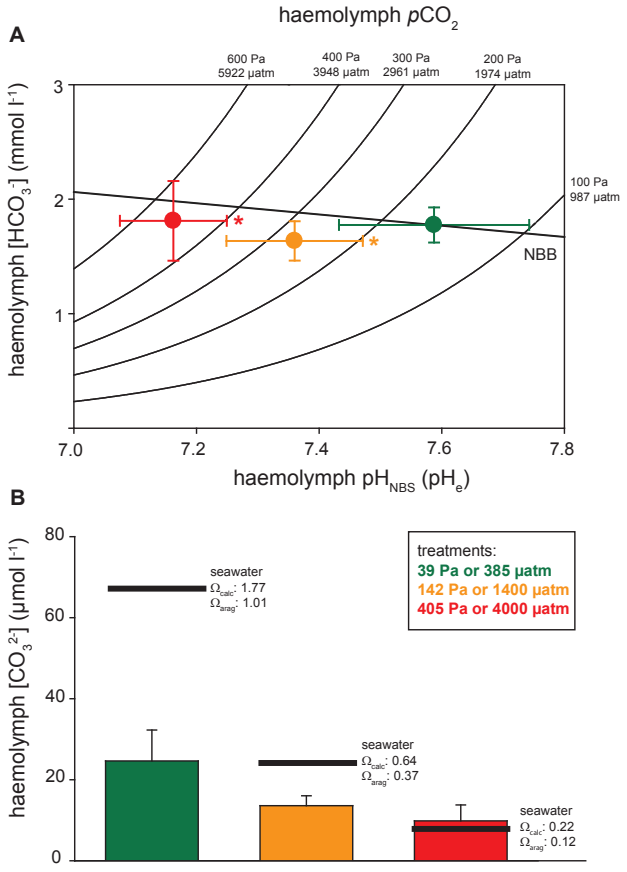

Fig. 3. (A) haemolymph acid-base status in relation to environmental pCO_2 (Davenport-diagram) for treatment groups at pCO_2 levels of 39 Pa (385 µatm, N = 12), 142 Pa (1400 µatm, N = 12) and 405 Pa (4000 µatm, N = 6). Isobars represent haemolymph pCO_2. NBB = non-bicarbonate buffer line. Mussels cannot significantly elevate $[HCO_3^-]$ to compensate pH_e. See also Table S1A (Supplement) for ANOVA tables; **(B)** Calculated haemolymph $[CO_3^{2-}]$ at seawater pCO_2 values of 39, 142 and 405 Pa (385, 1400, 4000 µatm). Black lines indicate seawater $[CO_3^{2-}]$ and the corresponding $CaCO_3$ saturation state (Ω_{arag}).

observed at pCO_2 higher than ca. 180 Pa (ca. 1800 µatm). Clearly, acclimation, adaptation and food availability or quality could be responsible factors for the observed differences between both studies. Somatic growth was not significantly affected by pCO_2 in our experiment (Fig. 4f). This may primarily be due to high variability encountered between replicates, but also could point at a higher capacity for somatic growth vs. shell accretion under hypercapnic conditions. Findings pointing in this direction have recently been obtained for an echinoderm, where somatic growth was up-regulated under acidified conditions while calcification was suppressed (Gooding et al., 2009).

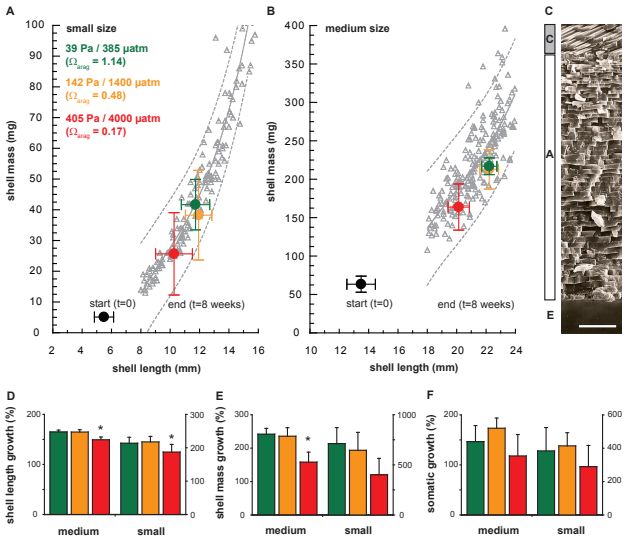

Fig. 4. **(A)** and **(B)** Shell mass vs. shell length relationships of small and medium experimental mussels at the beginning of the experiment (black) and after 8 weeks (red, orange, green; means and standard deviation). The grey symbols represent individual mussels from the collection site, the dashed line gives the 95% prediction interval for the shell mass vs. length relationship of wild mussels. **(C)** SEM cross-section of *M. edulis* shell (detail), showing the calcite (C) and aragonite (A) layers. Aragonite layers are in direct contact with the extrapallial fluid (EPF, E). Scale bar = 10 µm. **(D, E, F)** Percent shell mass and length, as well as somatic (dry mass) growth over the entire 8 week period. See Table S1 (Supplement) for ANOVA tables.

3.4 Shell microstructure and morphology (Exp. 2)

SEM analyses of shell cross-sections from mussels with a similar final length from all growth trial treatments (Table 4), illustrates that there are no significant changes in the thickness of the calcite and aragonite layers of the newly formed shell parts when pCO_2 is elevated. While calcite layer thickness is also comparable between 39 Pa and 405 Pa (385 and 4000 µatm) mussels, a significant decrease in the thickness of individual aragonite platelet layers, from 0.60 to 0.38 µm, was evident in the 405 Pa (4000 µatm) treatment. This indicates that high levels of acidification result in changes in shell microstructure that are not detected by simple shell mass vs. shell length regression analysis. As mentioned above, it needs to be emphasized that nacre (aragonite) platelet layers on the inner side of the shell (Fig. 4c) are in contact with an extrapallial fluid (EPF) that is most likely characterized by Ω_{arag} of below 0.4 even under present-day conditions. Our shell microstructure analysis (Table 4) indicates that even at 405 Pa (4000 µatm), the same number of aragonite platelets can be formed as in control animals of the same length. Thus, mussels possess a powerful calcification machinery to construct and maintain shell integrity in an EPF that is highly under saturated with $CaCO_3$.

Table 4. Shell microstructure analysis using SEM. N = 5 mussels of similar final length (medium size) were cross sectioned at 75 and 95% shell length. Mean values ± SD, significant differences from control (39 Pa, 385 µatm) in bold. Both cross sections are located in parts of the shell that have been newly formed during the experimental incubation.

Treatment (Pa or µatm)	Initial shell length (mm)	Final shell length (mm)	95% shell length	75% shell length			
			calcite thickness (µm)	calcite thickness (µm)	aragonite thickness (µm)	Layers of aragonite (*n*)	aragonite layer thickness (µm)
39 or 385	12.4 ± 1.8	21.4 ± 1.2	95.6 ± 14.0	99.2 ± 9.1	9.6 ± 2.8	15.8 ± 3.7	0.60 ± 0.11
142 or 1400	12.4 ± 1.3	21.2 ± 0.9	101.5 ± 17.3	87.4 ± 6.0	10.2 ± 6.2	15.4 ± 6.8	0.62 ± 0.13
405 or 4000	14.1 ± 0.5	21.1 ± 1.7	109.6 ± 19.2	99.7 ± 19.6	7.5 ± 6.2	17.2 ± 9.3	**0.38 ± 0.13**

SEM shell microstructure analysis of medium sized mussels.

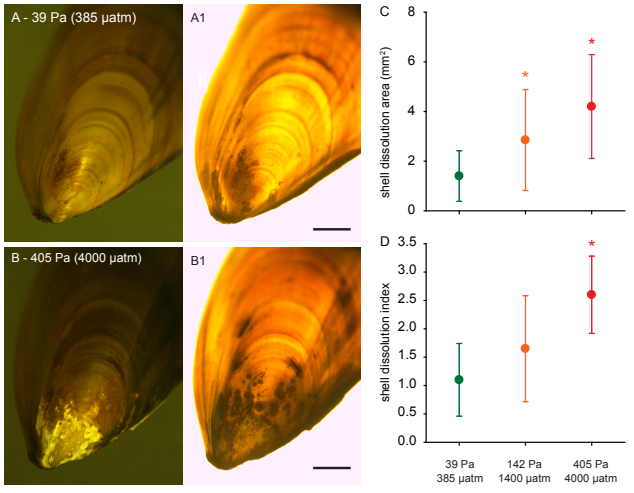

Fig. 5. External shell dissolution at the umbo region. Images of umbones of medium sized shells taken under reflected (A, B) and transmitted (A1, B1) illumination to quantify shell dissolution area and the severity. In B1, dissolution spots are visible as darker regions, as corroded shell material blocks the light more than intact crystal structures. (A, A1) 39 Pa (385 µatm), dissolution index = 1, (B, B1) 405 Pa (4000 µatm), dissolution index = 3; scale bars = 2.5 mm. (C) shell dissolution area at the umbo region (mm^2) of medium sized mussels, (D) shell dissolution index; N = 20 mussels randomly chosen from the 4 replicate treatments, asterisks indicate significant differences from control (39 Pa, 385 µatm) using Dunn's test. See Table S1 (Supplement) for the Kruskal-Wallis tests.

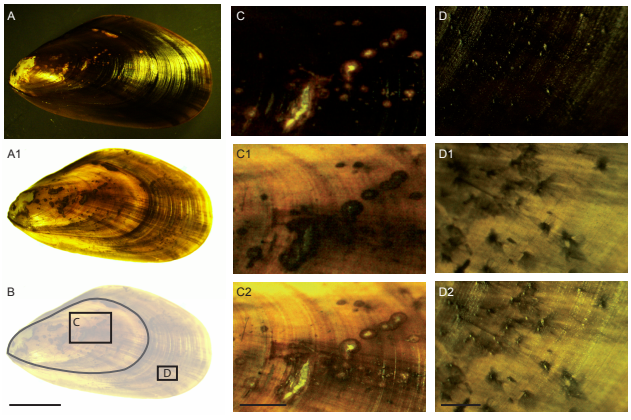

Fig. 6. Example of a medium sized mussel (405 Pa, 4000 µatm) with dissolution spots on old and newly formed parts of the shell. (A, A1) overview, reflected light (A), transmission light (A1). (B) position of close-up areas 1 (C) and 2 (D). Close up area 1 (C, C1, C2) is located on pre-experimental shell parts (black trace in C indicates the size of the mussel at the start of the experiment), close-up area 2 (D, D1, D2) on newly formed shell material. C, D are reflected light pictures, C1 and D1 are transmission images, C2 and D2 combined reflected and transmission images. White spots are corroded calcite / aragonite material that is visible when the periostracum is fractured. These spots appear dark when viewed under transmission light. Scale bars: A to C: 5 mm, D to F: 1 mm, G to I: 0.5 mm.

M. edulis seems to be well adapted to form shell material even under highly acidified conditions when the newly formed material is protected by an intact periostracum. The periostracum, composed of quinone-tanned scleroproteins, has been demonstrated to be resistant towards various chemicals (reviewed in Waite 1983). However, fractures of the periostracum seem to be fairly common, even in control mussels and especially at the umbo region and other older parts of the shell (Fig. 5). Mussels occur in dense beds in Kiel Fjord (see Fig. 1d) and the umbo region is often in close contact to other mussels or the substrate. Friction in a wave swept environment then probably causes an abrasion of the organic cover. Such fractures can then act as sites for external shell dissolution. Some degree of periostracum damage and/or shell dissolution was found at the umbo region in 58 out of 60 medium sized mussels analyzed from Exp. 2. Dissolution area was smallest ($<2\,mm^2$) in control mussels and significantly increased at 142 and 405 Pa (1400 and 4000 µatm)

(Fig. 5c). While shell damage was primarily restricted to periostracum abrasion in the control group (dissolution index = 1, Fig. 5a), significantly more calcite dissolution was observed in the 405 Pa (4000 µatm) group (dissolution index = 3, Fig. 5b and d). Dissolution spots (e.g. Fig. 6) could be demonstrated in a range of mussels at 39, 142 and 405 Pa (385, 1400 and 4000 µatm), mainly in older parts of the shell, indicating that periostracum damage and subsequent external dissolution also occurs in the natural habitat (Fig. 6). As the experimental mussels were not screened for periostracum damage prior to the experiment, it is difficult to assess the magnitude of shell dissolution during the incubation. Tunnicliffe et al. (2009) report that deep-sea vent mussels *Bathymodiolus brevior* in close proximity to low pH habitats do not show damages of the periostracum or repaired shell parts, whereas populations in high pH habitats are characterized by occasional periostracum damage. The authors therefore concluded that damage of the periostracum necessarily leads to fatal shell $CaCO_3$ dissolution in the low pH habitat (Tunnicliffe et al., 2009). In two mussels (one at 142 Pa (1400 µatm), one at 405 Pa (4000 µatm) in our experiment, external dissolution spots could also be witnessed in newly formed shell parts (Fig. 6). It is unclear whether elevated seawater pCO_2 itself can disrupt the protective function of the periostracum. Future studies need to take this possibility into consideration, especially during longer incubations.

4 Conclusions

In summary, our laboratory studies demonstrate that calcification in this economically and ecologically important bivalve species can be maintained at control rates even when seawater Ω_{arag} is lower than 0.5 (pCO_2 142 Pa, 1400 µatm). 56 to 65% of control calcification rates can be obtained at a seawater pCO_2 of 405 Pa (4000 µatm), a pCO_2 that is twice as high as that producing zero calcification in a study of a North Sea population (Gazeau et al., 2007). This could be due to physiological differences between North and Baltic Sea populations of *M. edulis*. However, the present study as well as previous ones indicate that it is more likely that long-term acclimation to elevated pCO_2 increases the ability to calcify in *Mytilus* spp. (Michaelidis et al., 2005; Ries et al., 2009). We also show evidence that uncompensated extracellular pH at moderately elevated pCO_2 (142 Pa, 1400 µatm) does not significantly impair growth and calcification, suggesting that there is no causal relationship between the acid-base status and metabolic depression in this species at levels of ocean acidification that can be expected in the next few hundred years (IPCC, 2007). Rather, we show in a companion study that moderate levels of acidification (pCO_2 113 to 240 Pa, 1120 to 2400 µatm) increase metabolic rates, potentially indicating increased costs for calcification and cellular homeostasis (Thomsen and Melzner, 2010).

While current levels of CO_2 enrichment may still permit the dominance of calcifying communities in habitats such as Kiel Fjord, future increases in pCO_2 could deplete their tolerance capacity: an increase in seawater pCO_2 from 39 to 78 Pa (385 to 770 µatm) due to future ocean acidification will elevate C_T by approximately 90 µmol kg^{-1} (at $S = 20$, A_T = 2060 µmol kg^{-1}, T = 20 °C), but leave A_T unaffected. Simple model calculations illustrate, how additional increases in C_T due to respiration in deeper water masses and subsequent upwelling would affect the speciation of the carbonate system in Kiel Fjord (Fig. 1b): adding 100 µmol kg^{-1} of C_T to the values measured in 2008 and 2009 (see Table 1) and leaving A_T unaltered results in a dramatic increase of pCO_2. Peak pCO_2 values would shift from ca. 230 to >440 Pa (>4300 µatm) and average pCO_2 would shift from ca. 104 Pa to 248 Pa (2450 µatm). As pCO_2 is generally highest in the summer months, mussel recruitment could be one of the first processes to be affected: Kurihara et al. (2009) demonstrated a high CO_2 sensitivity of larval *M. galloprovincialis*, with an increased prevalence of shell malformation at a pCO_2 of ca. 200 Pa (ca. 2000 µatm). Such values could be reached within the next decades in Kiel Bay (Fig. 1b). However, older mussels would probably be affected just as well: considering that abrasions of the periostracum are very common among *M. edulis* in Kiel Fjord, enhanced external shell dissolution may compromise fitness of older mussels during long-term exposure to seawater highly under saturated with $CaCO_3$ by negatively influencing shell stability. In addition, increased external shell dissolution might favour settlement of the shell boring polychaete *Polydora ciliata* which can more easily penetrate areas with a damaged periostracum (Michaelis, 1978). *P. ciliata* boring may render mollusc shells more vulnerable to crab predation (Blöcher 2008). In addition, invasion of the extracellular space by microorganisms through minute shell fractures seems possible. Long-term experiments (>6 months) are necessary to test these hypotheses.

Coastal upwelling habitats such as Kiel Bay or the West coast of the United States (Feely et al., 2008) can be important "natural analogues" to understand how ecosystems might be influenced by future ocean acidification. In contrast to a natural analogue study that shows a progressive displacement of calcifying organisms by photoautotrophic communities along a CO_2 gradient in the Mediterranean (Hall-Spencer et al., 2008), we show that communities dominated by calcifying invertebrates can thrive in CO_2 enriched (eutrophic, "energy dense") coastal areas. However, such habitats, which are quite common along the world's coasts (Diaz and Rosenberg, 2008), will be exposed to rates of change in seawater pCO_2 that go well beyond the worst scenarios predicted for surface oceans (Caldeira and Wickett, 2003).

Supplementary material related to this article is available online at: http://www.biogeosciences.net/7/3879/2010/bg-7-3879-2010-supplement.pdf.

Acknowledgements. The authors wish to thank Ulrike Panknin for culturing algae, supervising the long-term experiment, and laboratory work associated with this project, Hans-Ulrik Riisgard (University of Southern Denmark) for his suggestion on how to improve filtration efficiency and experimental design, Renate Schütt for marking mussels with $MnCl_2$ and carrying out the settlement plate work and Susann Grobe for carbonate chemistry analysis. This study was funded by DFG Excellence Cluster "Future ocean" grants to AK, FM and MW. This work is a contribution to the German Ministry of Education and Research (BMBF)-funded project "Biological Impacts of Ocean ACIDification"(BIOACID) subproject 3.1.3 awarded to FM and MAG and is a contribution to the "European Project on Ocean Acidification" (EPOCA) that received funding from the European Community's Seventh Framework Programme (FP7/2007 to 2013) under grant agreement no 211384.

Edited by: J.-P. Gattuso

References

Albers, C. and Pleschka, K.: Effect of temperature on CO_2 transport in elasmobranch blood, Resp. Phys., 2, 261–273, 1967.

Barbin, V., Ramseyer, K., and Elfman, M.: Biological record of added manganese in seawater: a new efficient tool to mark in vivo growth lines in the oyster species *Crassostrea gigas*, Int. J. Earth. Sci., 97, 193–199, 2008.

Blöcher, N.: Ökologische und biologische Aspekte des *Polydora ciliata* – Aufwuchses auf *Littorina littorea*, MSc Thesis, University of Kiel, 2008.

Booth, C. E., McDonald, D. G., and Walsh, P. J.: Acid-base-balance in the sea mussel, *Mytilus-edulis*, 1. Effects of hypoxia and air-exposure on hemolymph acid-base status, Mar. Biol. Lett., 5, 347–358, 1984.

Bradford, M. M.: Rapid and sensitive method for quantitation of microgram quantities of protein utilizing principle of protein-dye binding, Anal. Biochem., 72, 248–254, 1976.

Caldeira, K. and Wickett, M. E.: Anthropogenic carbon and ocean pH, Nature, 425, 365–365, 2003.

Diaz, R. J. and Rosenberg, R.: Spreading dead zones and consequences for marine ecosystems, Science, 321, 926–929, 2008.

Dickson, A. G. and Millero, F. J.: A comparison of the equilibrium-constants for the dissociation of carbonic-acid in seawater media, Deep-Sea Res., 34, 1733–1743, 1987.

Dickson, A. G.: Standard potential of the reaction – $AgCl_S$+1/2 H_2 = Ag_S+HCl_{Aq} and the standard acidity constant of the ion HSO_4 – in synthetic sea-water from 273.15-K to 318.15-K, J. Chem. Thermodyn., 22, 113–127, 1990.

Dickson, A. G., Afghan, J. D., and Anderson, G. C.: Reference materials for oceanic CO_2 analysis: a method for the certification of total alkalinity, Mar. Chem., 80, 185–197, 2003.

Dickson, A. G., Sabine, C. L., and Christian, J. R.: Guide to best practices for ocean CO_2 measurements PICES Special Publications, 191 pp., 2007.

Dupont, S., Havenhand, J., Thorndyke, W., Peck, L., and Thorndyke, M.: Near-future level of CO_2-driven ocean acidification radically affects larval survival and development in the brittlestar *Ophiothrix fragilis*, Mar. Ecol.-Prog. Ser., 373, 285–294, 2008.

Dürr, S. and Wahl, M.: Isolated and combined impacts of blue mussels (*Mytilus edulis*) and barnacles (*Balanus improvisus*) on structure and diversity of a fouling community, J. Exp. Mar. Biol. Ecol., 306, 181–195, 2004.

Enderlein, P. and Wahl, M.: Dominance of blue mussels versus consumer-mediated enhancement of benthic diversity, J. Sea Res., 51, 145–155, 2004.

Fabry, V. J., Seibel, B. A., Feely, R. A., and Orr, J. C.: Impacts of ocean acidification on marine fauna and ecosystem processes, ICES J. Mar. Sci., 65, 414–432, 2008.

Feely, R. A., Sabine, C. L., Hernandez-Ayon, J. M., Ianson, D., and Hales, B.: Evidence for upwelling of corrosive "acidified" water onto the continental shelf, Science, 320, 1490–1492, 2008.

Gazeau, F., Quiblier, C., Jansen, J. M., Gattuso, J. P., Middelburg, J. J., and Heip, C. H. R.: Impact of elevated CO_2 on shellfish calcification, Geophys. Res. Lett., 34, L07603, 2007.

Gooding, R. A., Harley, C. D. G., and Tang, E.: Elevated water temperature and carbon dioxide concentration increase the growth of a keystone echinoderm, P. Natl. Acad. Sci. USA, 106, 9316–9321, 2009.

Gutowska, M. A. and Melzner, F.: Abiotic conditions in cephalopod (*Sepia officinalis*) eggs: embryonic development at low pH and high pCO_2, Mar. Biol., 156, 515–519, 2009.

Gutowska, M. A., Melzner, F., Langenbuch, M., Bock, C., Claireaux, G., and Portner, H. O.: Acid-base regulatory ability of the cephalopod (*Sepia officinalis*) in response to environmental hypercapnia, J. Comp. Physiol. B, 180, 323–335, 2010.

Hall-Spencer, J. M., Rodolfo-Metalpa, R., Martin, S., Ransome, E., Fine, M., Turner, S. M., Rowley, S. J., Tedesco, D., and Buia, M. C.: Volcanic carbon dioxide vents show ecosystem effects of ocean acidification, Nature, 454, 96–99, 2008.

Hansen, H. P., Giesenhagen, H. C., and Behrends, G.: Seasonal and long-term control of bottom-water oxygen deficiency in a stratified shallow-water coastal system, ICES J. Mar. Sci., 56, 65–71, 1999.

IPCC: Climate Change 2007: The Physical Science Basis. Contribution of Working Group I to the Fourth Assessment Report of the Intergovernmental Panel on Climate Change, Cambridge University Press, Cambridge, United Kingdom and New York, NY, USA, 2007.

Ismar, S. M. H., Hansen, T. and Sommer, U.: Effect of food concentration and type of diet on *Acartia* survival and naupliar development, Mar. Biol., 154, 335–343, 2008.

Kossak, U.: How climate change translates into ecological change: Impacts of warming and desalination on prey properties and predator-prey interactions in the Baltic Sea, Ph.D. dissertation, IFM-GEOMAR, Christian-Albrechts-Universität, Kiel, 97 pp., 2006.

Kurihara, H.: Effects of CO_2-driven ocean acidification on the early developmental stages of invertebrates, Mar. Ecol.-Prog. Ser., 373, 275–284, 2008.

Kurihara, H., Asai, T., Kato, S., and Ishimatsu, A.: Effects of elevated pCO_2 on early development in the mussel Mytilus galloprovincialis, Aquat. Biol., 4, 225–233, 2009.

Lehmann, A., Krauss, W., and Hinrichsen, H. H.: Effects of remote and local atmospheric forcing on circulation and upwelling in the Baltic Sea, Tellus A, 54, 299–316, 2002.

Lindinger, M. I., Lauren, D. J., and McDonald, D. G.: Acid-base-balance in the sea mussel, *Mytilus edulis*, 3. Effects of environmental hypercapnia on intracellular and extracellular acid-base-balance, Mar. Biol. Lett., 5, 371–381, 1984.

Mehrbach, C., Culberso, C. H., Hawley, J. E., and Pytkowic, R. M.: Measurement of apparent dissociation-constants of carbonic-acid in seawater at atmospheric-pressure, Limnol. Oceanogr., 18, 897–907, 1973.

Melzner, F., Gutowska, M. A., Langenbuch, M., Dupont, S., Lucassen, M., Thorndyke, M. C., Bleich, M., and Pörtner, H.-O.: Physiological basis for high CO_2 tolerance in marine ectothermic animals: pre-adaptation through lifestyle and ontogeny?, Biogeosciences, 6, 2313–2331, doi:10.5194/bg-6-2313-2009, 2009.

Michaelidis, B., Ouzounis, C., Paleras, A., and Pörtner, H. O.: Effects of long-term moderate hypercapnia on acid-base balance and growth rate in marine mussels *Mytilus galloprovincialis*, Mar. Ecol.-Prog. Ser., 293, 109–118, 2005.

Michaelis, M.: Zur Morphologie und Ökologie von *Polydora ciliata* und *P. ligni* (Polychaeta, Spionidae), Helgoland, Wiss. Meer., 31, 102–116, 1978.

Mintrop, L., Perez, F. F., Gonzalez-Davila, M., Santana-Casiano, M. J., and Körtzinger, A.: Alkalinity determination by potentiometry: Intercalibration using three different methods, Cienc. Mar., 26, 23–37, 2000.

Misogianes, M. J. and Chasteen, N. D.: Chemical and Spectral Characterization of the Extrapallial Fluid of Mytilus-Edulis, Anal. Biochem., 100, 324–334, 1979.

Nikulina, A., Polovodova, I., and Schönfeld, J.: Foraminiferal response to environmental changes in Kiel Fjord, SW Baltic Sea, eEarth, 3, 37–49, doi:10.5194/ee-3-37-2008, 2008.

Pörtner, H. O., Langenbuch, M., and Reipschläger, A.: Biological impact of elevated ocean CO_2 concentrations: Lessons from animal physiology and earth history, J. Oceanogr., 60, 705–718, 2004.

Reusch, T. B. H. and Chapman, A. R. O.: Persistence and space occupancy by subtidal blue mussel patches, Ecol. Monogr., 67, 65–87, 1997.

Ries, J. B., Cohen, A. L., and McCorkle, D. C.: Marine calcifiers exhibit mixed responses to CO_2-induced ocean acidification, Geology, 37, 1131–1134, 2009.

Riisgard, H. U., Kittner, C., and Seerup, D. F.: Regulation of opening state and filtration rate in filter-feeding bivalves (*Cardium edule*, *Mytilus edulis*, *Mya arenaria*) in response to low algal concentration, J. Exp. Mar. Biol. Ecol., 284, 105–127, 2003.

Roy, R. N., Roy, L. N., Vogel, K. M., Porter-Moore, C., Pearson, T., Good, C. E., Millero, F. J., and Campbell, D. M.: The dissociation constants of carbonic acid in seawater at salinities 5 to 45 and temperatures 0 to 45 °C, Mar. Chem., 44, 249–267, 1993.

Suzuki, M., Saruwatari, K., Kogure, T., Yamamoto, Y., Nishimura, T., Kato, T., and Nagasawa, H.: An acidic matrix protein, Pif, is a key macromolecule for nacre formation, Science, 325, 1388–1390, 2009.

Thomsen, J. and Melzner, F.: Seawater acidification does not elicit metabolic depression in the blue mussel *Mytilus edulis*, Mar. Biol., 157, 2667–2676, doi:10.1007/s00227-010-1527-0, 2010.

Tunnicliffe, V., Davies, K. T. A., Butterfield, D. A., Embley, R. W., Rose, J. M., and Chadwick Jr, W. W.: Survival of mussels in extremely acidic waters on a submarine volcano, Nat. Geosci., 2, 344–348, 2009.

Waite, J. H.: Quinone-tanned scleroproteins, in: The Mollusca, Vol. 1, Metabolic biochemistry and molecular biomechanics, edited by: Hochachka, P. W., 467–504, 1983.

Weiss, I. M.: Jewels in the pearl, ChemBioChem., 11, 297–300, 2010.

Weiss, R. F.: Carbon dioxide in water and seawater: the solubility of a non-ideal gas, Mar. Chem., 2, 203–215, 1974.

Yin, Y., Huang, J., Paine, M. L., Reinhold, V. N., and Chasteen, N. D.: Structural characterization of the major extrapallial fluid protein of the mollusc *Mytilus edulis*: Implications for functions, Biochemistry, 44, 10720–10731, 2005.